AIAA JOURNAL
Vol. 32, No. 1, January 1994

Active Control of Fan Noise from a Turbofan Engine

Russell H. Thomas,* Ricardo A. Burdisso,† Christopher R. Fuller,‡ and Walter F. O'Brien§
Virginia Polytechnic Institute and State University, Blacksburg, Virginia 24061

A three-channel active control system is applied to an operational turbofan engine to reduce tonal noise produced by both the fan and the high-pressure compressor. The control approach is the feedforward filtered-x least-mean-square algorithm implemented on a digital signal processing board. Reference transducers mounted on the engine case provide blade passing and harmonics frequency information to the controller. Error information is provided by large area microphones placed in the acoustic far field. To minimize the error signal, the controller actuates loudspeakers mounted on the inlet to produce destructive interference. The sound pressure level of the fundamental tone of the fan was reduced using the three-channel controller by up to 16 dB over a ±30-deg angle about the engine axis. A single-channel controller could produce reduction over a ±15-deg angle. The experimental results show the control to be robust. Outside of the areas controlled, the levels of the tone actually increased due to the generation of radial modes by the control sources. Simultaneous control of two tones is achieved with parallel controllers. The fundamental and the first harmonic tones of the fan were controlled simultaneously with reductions of 12 and 5 dBA, respectively, measured on the engine axis. Simultaneous control was also demonstrated for the fan fundamental and the high-pressure compressor fundamental tones.

Nomenclature

$C(\ )$ = cost function
D = diameter of the engine fan, 0.53 m
d_k = disturbance signal
$E[\ ]$ = expected value operator
e_k = error signal
T = transfer function
u_k = control source input signal
w_i = adaptive filter coefficients
x_k = reference signal
y_k = control source output signal
γ = coherence
μ = convergence parameter

Introduction

NOISE has been a significant negative factor associated with the commercial airline industry since the introduction of the aircraft gas turbine engine. As engines evolved from turbojet to primarily turbofan cycles, fan noise has become an increasingly large contributor of total engine noise. For high bypass ratio engines (with bypass ratios of 5 to 6) currently in use, fan noise dominates the total noise on approach.[1] On takeoff, the fan exhaust noise and the jet noise can both be the dominant noise sources.[1] Traditionally, acoustic wall treatment has been used as a method to address this problem. However, this passive technique has only made small reductions in total fan inlet noise levels of less than 5 perceived noise level (PNL) dB,[1] although for a specific tone the reductions can be greater. A typical fan acoustic spectrum includes a broadband noise level and tones at the blade passage frequency and its harmonics. These tones, for narrowband measurements, are usually 10–15 dB above the broadband level. This is for the case where the fan tip speed is subsonic. Multiple pure tones appear as the tip speed becomes supersonic.

The introduction of ultrahigh-bypass ratio engines in the future, with the bypass ratios in the range of 10 or greater, will result in a greater fan noise component although the inherent overall noise level may be less than current high-bypass ratio engines. It is also reasonable to expect that the noise requirements will grow increasingly stringent such that even ultrahigh-bypass engines will have difficulty meeting them. Also, with shorter inlet ducts relative to the size of the fan and for the lower blade passage frequencies expected for these engines, passive acoustic liners will have greater difficulty attenuating fan tones because liners are less effective as the frequencies decrease and the acoustic wavelength increases. Because of these difficulties, it is likely that passive fan tone control techniques, although continuing to progress, will be combined with active noise control techniques to produce an effective noise control solution for fans.

For subsonic tip speed fans, noise is produced by the interaction of the unsteady flows and solid surfaces.[2–4] This could result from inflow disturbances such as the inlet boundary layer interacting with the rotor or the rotor wakes interacting with the stator vanes. Acoustic mode coupling and propagation in the duct and, in turn, acoustic coupling to the far field determines the net far-field acoustic directivity pattern.

Reduction of the disturbance noise field from the fan of a turbomachine can be achieved by either cancellation at the source or superposition of an out-of-phase secondary noise field. Reduction at the source entails focusing on modifying the incident aerodynamic unsteadiness or the resulting blade response and unsteady lift, or modifying the mode generation and propagation from such interactions.[4–8] Most efforts at noise reduction in this area are passive in nature, in that the attenuation is obtained by the permanent alteration of the system. Examples include the effects of respacing the rotor and stator[9] and the spacing of the rotor and downstream struts.[10]

However, there have been some efforts at active control of these source mechanisms. Preliminary experiments have shown the attenuation of noise resulting from an incident gust on an airfoil by actuating a trailing edge flap to control the unsteady lift.[11] In general, an attempt to alter source mechanisms will require engine redesign, and the effect on performance will have to be assessed.

Of course, for commercial engines, efforts at reductions in source noise to date have been insufficient in reducing overall

Received Nov. 3, 1992; presented as Paper 93-0597 at the AIAA 31st Aerospace Sciences Meeting, Reno, NV, Jan. 11–14, 1993; revision received May 10, 1993; accepted for publication May 11, 1993.

*Research Scientist, Mechanical Engineering Department. Member AIAA.
†Assistant Professor, Mechanical Engineering Department.
‡Professor, Mechanical Engineering Department. Associate Fellow AIAA.
§J. B. Jones Professor and Associate Dean of Engineering, Mechanical Engineering Department. Associate Fellow AIAA.

engine noise levels to the required levels. The additional reductions have been met with passive engine duct liners. The contribution of duct liners is primarily in attenuating fan exhaust noise where the propagating modes have a higher order and propagate away from the engine axis where liners can be most effective. In the fan inlet, the modes are propagating against the boundary layer and are refracted toward the engine axis, minimizing the effectiveness of liners.

Another option for turbofan noise reduction is to actively control the disturbance noise field with a second control noise field. The concept of active sound control, or antinoise as it is sometimes referred to, is attributed to Paul Leug.[12] The principle behind active control of noise is the use of a control noise to destructively interfere with the disturbance noise.

While Leug's patent is almost 60 years old, only in the past 10–20 years has active control begun to emerge in many applications.[13–16] The applications of active control were made possible by the advancements in digital signal processing and in the development of adaptive control algorithms such as the very popular least-mean-square (LMS) algorithm.[17,18]

To produce an effective reduction in turbofan engine noise, reductions in both broadband noise levels and engine tone levels are desirable. Feasibility studies of the application of active noise control using secondary sources to reduce turbofan engine inlet noise have only recently been investigated.[19–21] This research has concentrated on fan tone noise exclusively, controlling the fan noise from a JT15D turbofan engine using an adaptive filtered-x LMS algorithm. A single-channel control system was used to control the fan blade passage frequency tone[19] and the blade-passage-frequency (BPF) tone and the first harmonic of the BPF tone,[20] for a plane wave excitation. A multichannel control system was used to control the first spinning mode.[21] The use of the multichannel control system to control both fan tones and a high-pressure compressor BPF tone for a plane wave excitation is the subject of this paper.

Experimental Apparatus and Method

The approach is to experimentally implement an adaptive feedforward active noise control system on an operational turbofan engine. The system reduces the level of a tone produced by the engine by the destructive interference of a control and disturbance sound fields. The active control system has four main components. A reference sensor provides a coherent signal with information on the frequency of the disturbance tone; this signal is fed forward to the adaptive filters that generate the control signals. Error sensors are placed in the acoustic far field of the engine to measure the resultant noise.

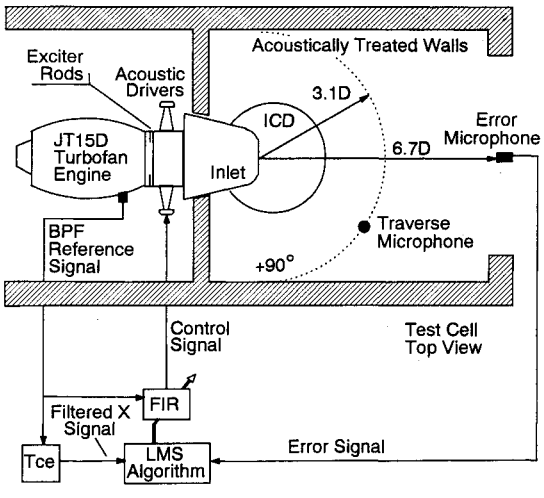

Fig. 1 Schematic diagram of JT15D engine in the test cell with active control system components; single channel control system represented.

The control algorithm takes input from the reference and error sensors and drives, by changing the coefficients of the adaptive filter, the control sound sources to minimize the signals from the error sensors. The control sound sources are compression drivers mounted on the inlet of the engine. A realistic application will require a light, compact sound source. This is a topic of additional research. A schematic of the engine, test cell, and the components of the controller are shown in Fig. 1 and will be discussed in detail in the next three sections. In Fig. 1, a single-input-single-output (SISO) controller is shown for simplicity. Most of the results in this work were obtained with a multiple-channel controller which will be described in following sections.

Engine and Test Cell

A Pratt and Whitney of Canada JT15D-1 turbofan engine is mounted in a test cell configuration at Virginia Polytechnic Institute and State University (VPI&SU). The JT15D engine is sized for an executive jet class of aircraft. It is a twin spool turbofan engine with a full-length bypass duct and a maximum bypass ratio of 2.7. There is a single-stage axial flow fan with 28 blades and a centrifugal high-pressure compressor with 16 full vanes and 16 splitter vanes. There are no inlet guide vanes and the diameter at the fan stage location is 0.53 m. The maximum rotational speed of the low-pressure spool is 16,000 rpm and 32,760 rpm for the high-pressure spool. The fan has a pressure ratio of 1.5 and a hub-to-tip ratio of 0.41. The low-pressure stator assembly following the fan consists of an outer stator in the bypass duct which has 66 stators. The number of stators and the position of the core stator is the only alteration from the production version. The core stator has 71 vanes replacing the 33 vanes of the production engine. Also, in this research engine the core stator is repositioned downstream to a distance of 0.63 fan-blade-root-chords from the fan blade root as compared to 0.28 chords for the production version. This was done in earlier work at NASA Langley Research Center for the purpose of having the fan-rotor-core-stator interaction tone cutoff and to reduce the broadband noise.[22] The acoustics of this particular engine have been substantially studied and reported.[22–24]

The engine is equipped with an inflow control device (ICD) mounted on the inlet. This ICD was built at VPI&SU using a NASA design.[25] The purpose of the ICD is to minimize the spurious effects of ground testing on acoustic measurements. Atmospheric turbulence and the ground vortex associated with testing an engine statically on the ground are stretched by the contraction of flow into the engine, and this generates strong tone noise by the fan which is unsteady and not present in flight. The ICD is a honeycomb structure which breaks up incoming vortices. The honeycomb is 5 cm thick, and the cells are aligned with streamlines calculated from a potential flow analysis. The ICD was found to produce a minimum pressure drop and negligible acoustic transmission losses.[25] In the current facility, however, the acoustic transmission characteristics were not measured. There was also no redirection of acoustic directivity and no new acoustic sources created.[25] This ICD was also designed to be more compact than inflow control devices available at that time. The maximum diameter is equivalent to 2.1 engine inlet diameters. An ICD of this type is particularly important when an engine is mounted very close to the ground as in this case, $1.3D$.

The engine is mounted in a test cell which is divided by a wall so that the forward section of the test cell is a semi-anechoic chamber where only the inlet of the engine is inside the chamber. The walls of the semi-anechoic chamber are covered with 7.6-cm-thick acoustic foam which minimizes reverberations and minimizes the influence of the noise from the jet of the engine. One wall of the semi-anechoic chamber is open to the atmosphere for engine intake air.

Active Control Apparatus

The 28 exciter rods, 0.48 cm in diameter and equally spaced circumferentially, were placed $0.19D$ upstream of the fan

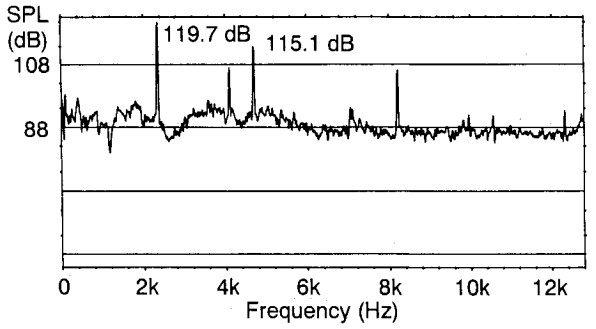

Fig. 2 Unfiltered spectrum of JT15D engine noise measured on the engine axis at a distance of 3.1*D*.

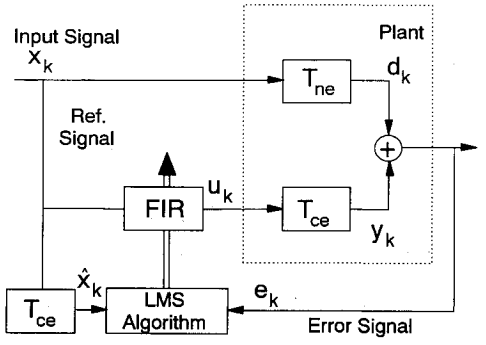

Fig. 3 Block diagram of filtered-*x* LMS algorithm.

stage. These rods extend 27% of the length of the fan blades through the outer casing into the flow. The wakes from the rods interact with the fan blades producing tones which are significantly higher in sound level than those produced without the interactions. The purpose of the rods is to excite an acoustic mode to dominance. With 28 rods, a number equal to the 28 fan blades, a plane wave mode is excited to dominance although higher order radial modes are also generated.[26] The plane wave mode has a uniform pressure amplitude over the inlet cross section and propagates at all frequencies beaming along the engine axis.[27]

A spectrum of the uncontrolled engine noise taken on the axis is shown in Fig. 2. It is marked by three significant tones in the audible range, the fan blade passage frequency (FBPF) tone at about 2360 Hz, the twice-fan blade passage frequency (2FBPF) tone at about 4720 Hz, and the high-pressure blade passage frequency (HPBPF) tone at about 4100 Hz. These frequencies correspond to the idle operating condition of the engine with the low-pressure spool at 31% of full speed and the high-pressure spool at 46% of full speed. The engine was run at idle condition for all of the experiments so that these three tones would be in the audible range and, for the frequencies involved, all three tones would be within the computational speed requirements of the controller.

The reference signals which are required by the feedforward controller are produced by two sensors mounted on the engine. One sensor is mounted flush with the casing at the fan stage location. This eddy-current sensor picks up the passage of each fan blade and provides a very accurate time history measure of the blade passage frequency of the fan. The signal also contains several harmonics of the FBPF which is used, with filtering, to provide a reference for the 2FBPF tone. The second reference sensor must provide the blade passage frequency of the high-pressure compressor. To install an eddy-current sensor, as described earlier, disassembly of the engine would be required. To avoid this, a sensor was installed on the tachometer shaft which is accessible from the accessory gearbox. The tachometer shaft has a geared direct drive from the high-pressure spool. The reference sensor consists of a gearbox driving a wheel with 99 holes such that the passage of each hole corresponds to the passage of a blade on the high-pressure compressor. An optical sensor produces a signal with each hole passage. By filtering this signal, an accurate time history of the HPBPF tone is obtained.

The loudspeakers attached to the circumference of the inlet are the control sound sources. They are actuated by the controller producing the secondary control sound field which interferes with and reduces the engine tonal noise. Two loudspeakers are attached to each horn for a total of 12 horns and 24 loudspeakers. The loudspeakers are commercially available 8-ohm drivers capable of 100 W on a continuous program with a flat frequency response to within 2 dB from 2 to 5 kHz. The horns have a throat diameter of 1.9 cm with an exponential flare in the direction of flow in the inlet. The opening of the horn in the inlet wall is 1.9 cm × 7.6 cm.

Error sensors are the last component of the active control hardware. They measure the resultant noise of the engine and control sound sources. A particular mode of engine noise can be highly directional and unsteady. The engine sound radiation pattern is characterized by the presence of lobes and acoustic notches. The spatial direction of these notches are probably subjected to small perturbations in the experimental setup. The placement of point error microphones near these directions results in an unsteady error signal as observed experimentally. To overcome this problem, a large area transducer was devised that spatially averages the incident sound pressure. These error sensors were made of a polyvinyldine-fluoride (PVDF) film 7.6 cm in diameter. The film was flat and backed with foam. The foam is approximately 5 cm thick and is inserted in a round PVC pipe open on both ends. These large-area PVDF microphones are uncalibrated and produce a relative measurement of sound pressure level. Since the control system has an equal number of control and error channels, each error sensor signal is driven theoretically toward zero and thus no calibration is required.

Active Control Algorithm

A block diagram of a single-channel filtered-*x* LMS control algorithm is shown in Fig. 3 (see Ref. 28). The resultant signal from the plant is the error signal e_k, which is the combination of the disturbance signal d_k and the signal due to the control source y_k

$$e_k = d_k + y_k \tag{1}$$

where the subscript k indicates a signal sample at time t_k. The response due to the control sources y_k can be replaced in terms of the input to the control sources u_k and the transfer function between the control input and its response at the error sensor y_k as

$$e_k = d_k + T_{ce}(k) * u_k \tag{2}$$

where the $*$ operator denotes a convolution. $T_{ce}(k)$ represents a causal, shift-invariant system such that the convolution can be found from the following convolution sum[29]

$$T_{ce}(k) * u_k = \sum_{n=0}^{\infty} T_{ce}(n) u_{k-n} \tag{3}$$

The input to the control sources u_k is the result of filtering the reference signal through the adaptive finite impulse response (FIR) filter. The control input becomes

$$u_k = w_k * x_k \tag{4}$$

$$u_k = \sum_{i=0}^{L} w_i x_{k-i} \tag{5}$$

where w_i are the adaptive coefficients of an Lth-order FIR filter.

Using Eqs. (4) and (2) the error signal becomes

$$e_k = d_k + T_{ce}(k) * w_k * x_k \tag{6}$$

The feedforward controller can only work when the reference signal is coherent to the disturbance signal. In this case, the filter output can be adapted to match the disturbance and the error signal can then be minimized. In fact, the maximum achievable reduction $R_{\max}$ of the error signal power is related to the coherence between x_k and d_k as[30]

$$R_{\max}(\text{dB}) = 10 \log[1/1 - \gamma_{xd}^2] \tag{7}$$

where γ_{xd} is the coherence between the reference signal x_k and the disturbance signal d_k.

To find the optimum filter weights, a cost function is defined using the error signal as

$$C(w_i) = E[e_k^2] \tag{8}$$

With the substitution of Eqs. (5) and (6), Eq. (8) becomes

$$C(w_i) = E\left[\left\{d_k + T_{ce}(k) * \left(\sum_{i=0}^{L} w_i x_{k-i}\right)\right\}^2\right] \tag{9}$$

The well-known LMS algorithm adapts the coefficients w_i $(i = 0, 1, \ldots, L)$ to minimize the cost function and thus, the error signal. The minimization is accomplished with a gradient descent method.[13] Differentiating the cost function in Eq. (8) with respect to a single weight w_i produces

$$\frac{\partial C}{\partial w_i} = 2E\left[e_k \frac{\partial e_k}{\partial w_i}\right] = 2E\left[e_k T_{ce}(k) * x_{k-i}\right] \tag{10}$$

The LMS approach further approximates the expected value operator by its instantaneous value as follows

$$\frac{\partial C}{\partial w_i} \approx 2e_k \hat{x}_{k-i} \tag{11}$$

The sequence $\hat{x}_k$ is referred to as the filtered-x signal, and is generated by filtering the reference signal x_k by an estimate of the control loop transfer function $T_{ce}(k)$. Obtaining $T_{ce}(k)$ is termed the system identification procedure. The FIR coefficient update using the filtered-x approach becomes

$$w_i(k+1) = w_i(k) - 2\mu e_k \hat{x}_{k-i} \qquad i = 1, \ldots, L \tag{12}$$

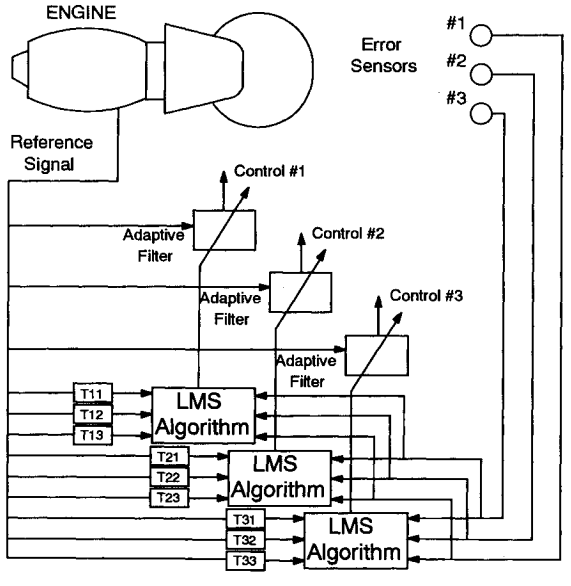

Fig. 4 Three-channel control system schematic.

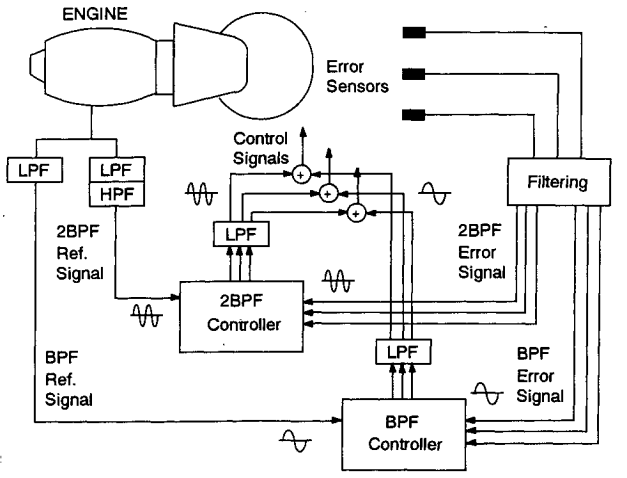

Fig. 5 Parallel control configuration; two controllers shown, each a three-channel system.

where μ governs the stability and rate of convergence. The second term of Eq. (12), $-2\mu e_k \hat{x}_{k-i}$, represents the change in the ith filter coefficient δw_i with each update. The change δw_i becomes smaller as the minimum is approached because the error signal is diminishing. For a constant rate of convergence, μ should increase as e_k decreases. A two-coefficient $(L = 1)$ FIR filter is needed to control a pure tone since they are sufficient to change the magnitude and phase of the control signal u_k.

A multiple-input-multiple-output (MIMO) controller with three control and three error channels was developed from the SISO system and is represented in Fig. 4. The approach is the same but the complexity has increased for the MIMO system as compared to the SISO controller. For clarity in the presentation, the derivation of the update equation is not presented here. However, the interested reader is referred to Ref. 31. The reference signal is fed forward to three adaptive FIR filters. Each filter has two coefficients and thus the phase and magnitude of the control signals can be adjusted independently. Each control signal is connected to the drivers attached to four consecutive horns. There are three error sensors which are placed in the acoustic far field. The cost function to be minimized is formed from the sum of the squares of the three error signals. It can be shown that there are now nine transfer functions to be measured to compute nine filtered-x signals.

By simply increasing the number of weights in the adaptive filters, the SISO and MIMO controllers can be extended to control multiple frequencies. However, this approach would impose a severe computational overhead to the controller and thus effectively reduce the frequency range. Another alternative was devised that overcomes this limitation. Recognizing that controlling tones of different frequencies is an uncoupled problem, a parallel configuration has been developed where multiple controllers work in parallel but are independently dedicated, one controller to each tone. This approach is illustrated in Fig. 5 for the case of the FBPF and its first harmonic. Each independent controller is a three-channel MIMO controller. Each controller can take reference information and error information from common sensors, appropriately filtered for each controller, or from different sets of sensors. The control output of the controllers is mixed and sent to the common set of control sound sources. This approach allows the sampling frequency and the rate of convergence of each controller to be optimized independently and allows flexibility in use of reference and error sensors.

All controllers were written in assembly language and implemented on a Texas Instrument TMS 320C30 digital signal processing board. The maximum sampling frequency for the MIMO controller is 29 kHz. For the first harmonic of the fan blade passage tone at 4700 Hz, the highest frequency tone

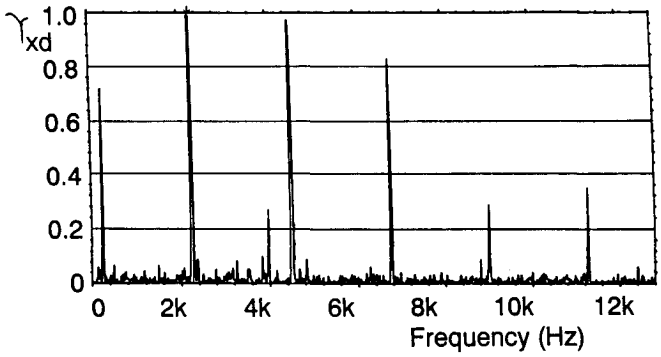

Fig. 6 Coherence measured between blade passage reference sensor and traverse microphone on engine axis at a distance of 3.1*D*.

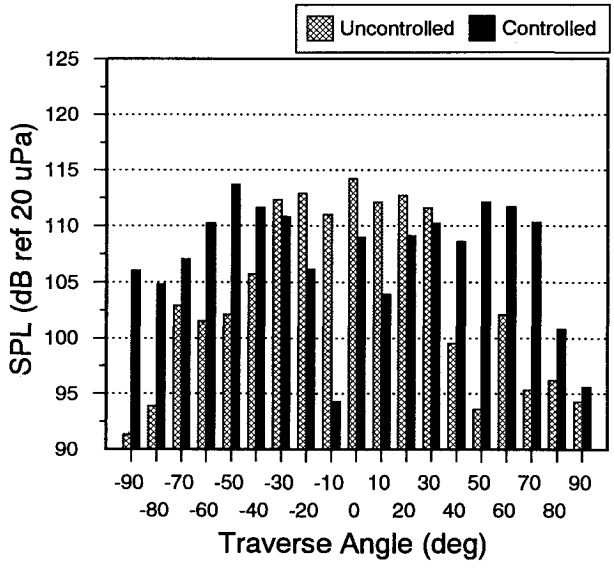

Fig. 7 Sound pressure level directivity for the fan blade passage tone uncontrolled and controlled with three-channel control system.

controlled, this sampling frequency would allow six samples per cycle and a filter coefficient update in real time.

Experimental Results

Before any active control system is implemented, the coherence between the reference and the error signal can be measured and, in conjunction with Eq. (7), an estimate of the expected reduction of the error signal can be obtained. A typical coherence measured between the fan reference sensor and the far-field error microphone is shown in Fig. 6. This shows very high coherence ($\gamma_{xd} > 0.96$ that gives $R_{\max} \simeq 14$ dB) both at the fundamental tone and at the first harmonic, which is essential to the feedforward controller. Coherence between the reference sensor on the high-pressure compressor and the far-field microphones was found to be similar.

A control experiment is performed in the following order. A system identification is obtained first by injecting an auxiliary tone at or near the frequency of the tone to be controlled and measuring the transfer functions between each channel of control sound sources and each error microphone. After this system identification is obtained, the controller is then initiated and converges to the optimum solution such that the tone is reduced at all three error microphones. A microphone is then traversed 180 deg at a distance of 3.1*D* to obtain the directivity of the tone in the horizontal plane of the engine axis. The traverse microphone is calibrated for measurement of the absolute sound pressure level. Several experiments were conducted and they are described in detail.

Control of Fan Blade Passage Frequency Tone

The three-channel MIMO controller was used to control the radiated sound at the FBPF tone at 2368 Hz. Three large-area PVDF microphones were used as error microphones and placed at a distance of 6.7*D* from the inlet lip. At this axial distance the error microphones 2, 1, and 3 were placed at −12, 0, and +12 deg, respectively, relative to the engine axis, and all three were in the horizontal plane through the engine axis.

The traverse microphone signal was fed to a spectrum analyzer where a 10-sample average was taken at each location on the traverse. The sound pressure levels of the FBPF tone before and after control were recorded and the resulting directivity plots are shown in Fig. 7. There is a zone of reduction where the sound pressure levels have been attenuated with the controller on as compared to uncontrolled levels. This zone of reduction extends from −30 to +30 deg with the attenuation levels varying from 1.4 dB at +30 deg to 16.7 dB at −10 deg. At angles greater than ±30 deg, toward the sideline regions, the sound pressure levels are higher with the controller as opposed to the uncontrolled levels. With three channels, and with this particular array of control sources, the controller does not have sufficient control over the directivity of the control sources. The engine noise has a high directivity forward in the angle from −35 to +35 deg. In other words, the controller and control sources have insufficient freedom to beam the control source noise in the forward angle, as the engine does, without increasing the sideline noise as well. This is expected to improve as the sophistication of the controller and control sources increases through a higher number of channels, improved algorithms, and optimum design and placement of the control drivers themselves.

Figure 8 shows the directivity for the same experiment, but at a FBPF of 2384 Hz, using a SISO controller with one large-area PVDF microphone placed on the axis. The area of reduction extends over a 30 deg sector from −20 to +10 deg which is a sector only one-half the 60-deg sector of sound pressure level reduction for the three-channel MIMO controller. Comparing sideline spillover for the MIMO and the SISO controllers, it is clear that going from one to three channels of control has reduced the sideline spillover somewhat. This demonstrates that by increasing the number of control channels improved global reduction is obtained.

For the three-channel experiment, everytime a data point was taken during the survey of the controlled sound field, a reading was taken from error sensor 1 which was located near the engine axis. This produced a time history of the error sensor which is shown in Fig. 9. After 9 min the controller was turned off and 9 min of data for the peak level of the uncon-

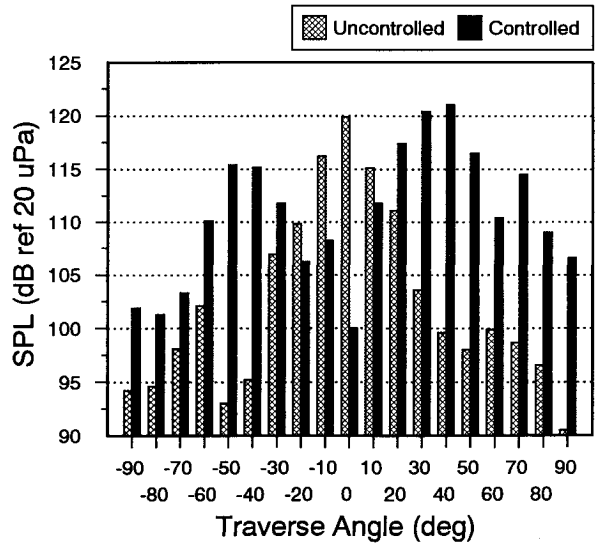

Fig. 8 Sound pressure level directivity for the fan blade passage tone uncontrolled and controlled with a single-channel control system.

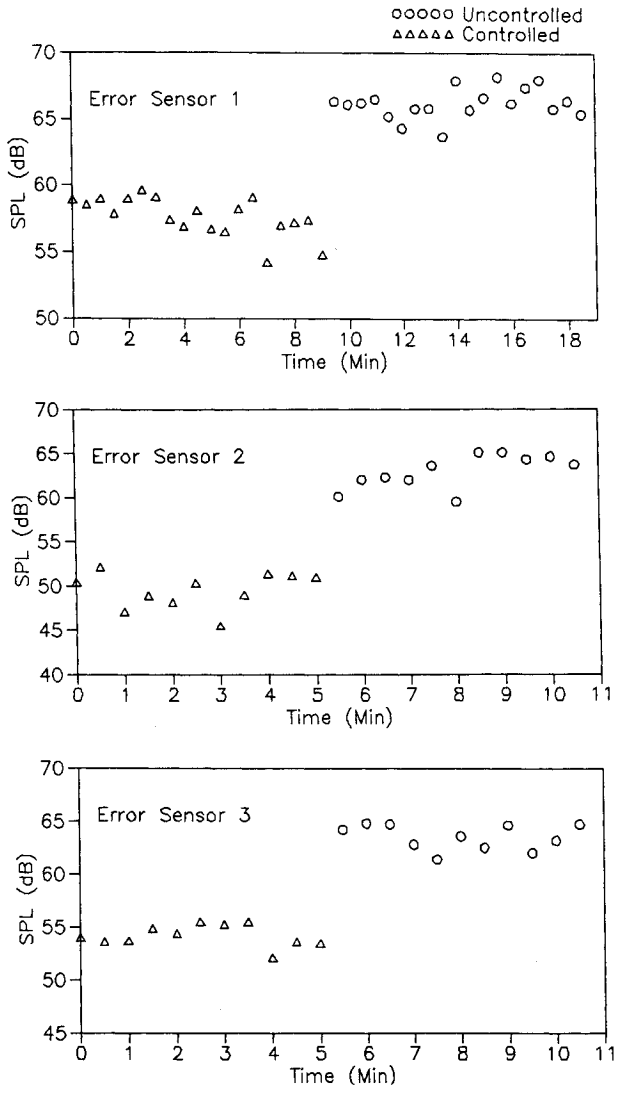

Fig. 9 Time history of error microphones for the three-channel control system measuring the peak value of the tone at the blade passage frequency.

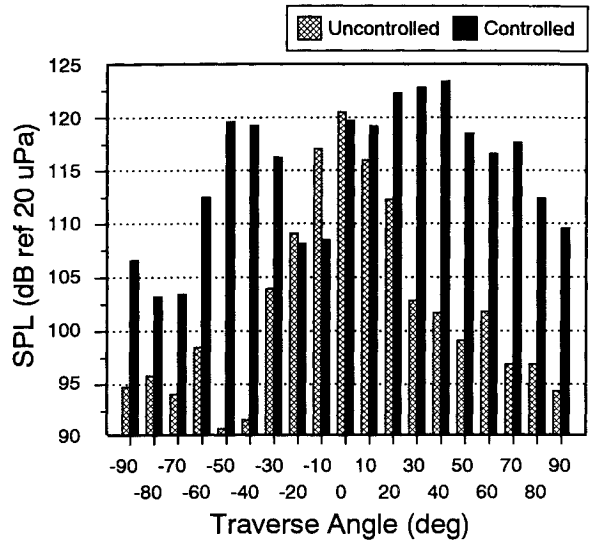

Fig. 10 Sound pressure level directivity of the fan blade passage tone uncontrolled and controlled with a single-channel system and a point error microphone.

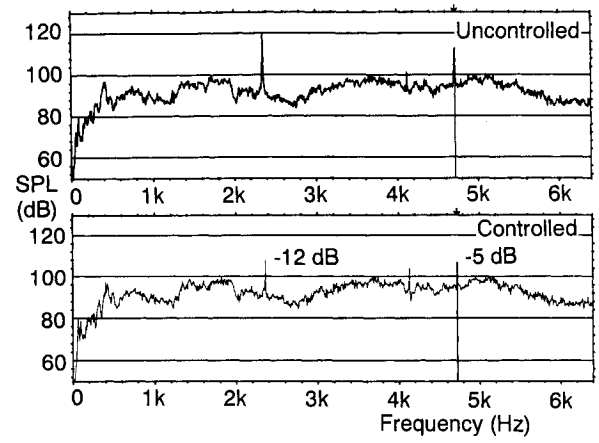

Fig. 11 Spectrum of traverse microphone on the engine axis, uncontrolled and demonstrating simultaneous control of the blade passage tone and the first harmonic.

trolled FBPF tone at error sensor 1 was taken. The controller was then turned on again to take 5 min of data each, controlled and uncontrolled, for error sensors 2 and 3. The time histories demonstrate the robustness of the controller in its ability to maintain control with time and, once a converged solution has been obtained, the ability of the controller to be switched on and off to achieve instantaneous control of an engine tone. These features work well as long as the system identification is valid. If the system identification were to change, the controller would need to have a new system identification and reconverge on the new solution to re-establish control.

The large-area PVDF microphones were developed for this research because of the inherent unsteadiness in the engine tonal noise directivity. A microphone distributed over a large area would be less sensitive to this unsteadiness than a conventional point microphone 1.2 cm in diameter, for example. Figure 10 for the FBPF of 2384 Hz shows the directivity using a SISO controller and one point error microphone placed at −10 deg. Comparison with Fig. 8 for a distributed microphone shows a larger area of reduction for the distributed microphone. A point microphone can only produce localized reduction or notches in the radiated sound.

Simultaneous Control of Engine Tones

Directivities of the three major tones in the audible range, FBPF, 2FBPF, and HPBPF show that on the engine axis at

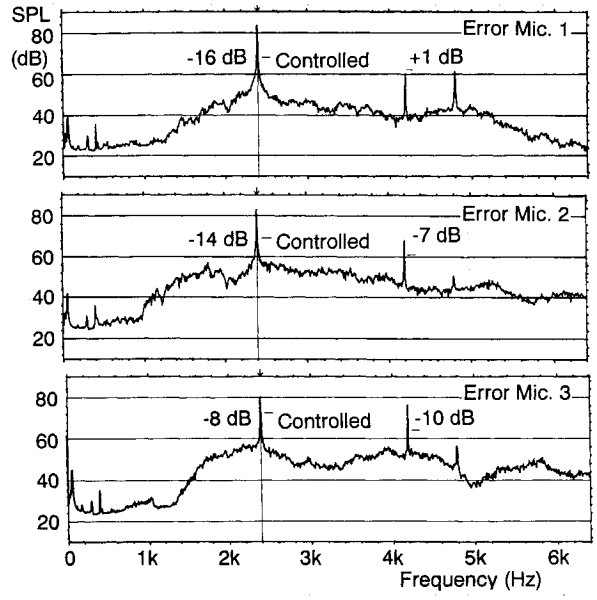

Fig. 12 Error microphone spectrums for three-channel control system demonstrating simultaneous control of fan blade passage frequency tone and high-pressure compressor blade passage frequency tone; controlled tone levels are indicated by the horizontal dashes.

0 deg, FBPF and 2FBPF are the dominant tones. For angles greater than ±10 deg, 2FBPF becomes the least of the three tones. Using the parallel MIMO control architecture of Fig. 5, simultaneous control of FBPF and 2FBPF tones was demonstrated. Three PVDF error microphones, 3, 1, and 2 were placed 6.4D from the engine inlet lip at +10, 0, and −13 deg, respectively, all in the horizontal plane.

The A-weighted spectrum of the traverse microphone at 0 deg is shown in Fig. 11, first for the uncontrolled case and then for the controlled case. The FBPF tone was reduced from 120 to 108 dBA with the controller on. The 2FBPF tone was reduced from 112 to 107 dBA. As noted previously, at 0 deg the HPBPF tone is insignificant.

The same control approach was used to control the FBPF tone and the HPBPF tone simultaneously. Error microphones 3, 1, and 2 were placed at a distance of 7.7D and at angles +9, 0, and −9 deg, respectively, in the horizontal plane. Figure 12 shows the spectrum from the three error microphones. These are filtered for use by the controller which is used to control the FBPF at 2400 Hz. Using the parallel control approach, the signal from the error sensors can be filtered differently for each controller. For control of the HPBPF tone, the signals shown in Fig. 12 would have an additional high pass filter at 3000 Hz. The FBPF tone is controlled at all three error sensor locations by between 8 and 16 dB of reduction. Notice that at error sensor 1 the HPBPF tone is much lower in level than it is at the other two locations. Therefore, the controller places less effort in controlling at that point and there is actually a 1-dB increase. At error microphones 2 and 3 the HPBPF tone is reduced by 7 and 10 dB, respectively.

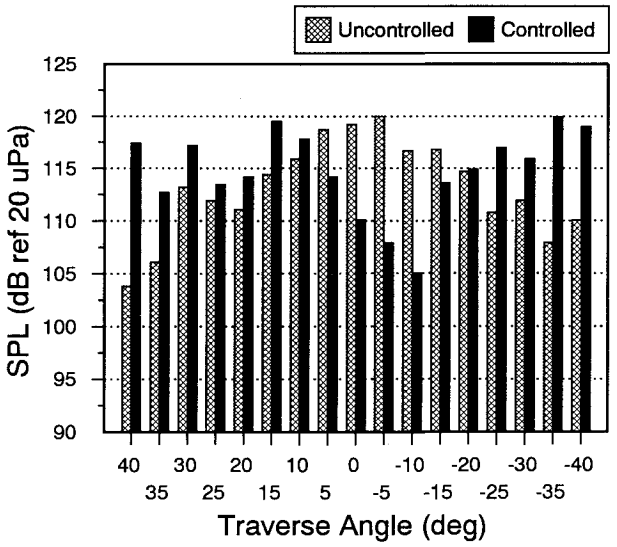

Fig. 13 Sound pressure level directivity of FBPF tone, uncontrolled and controlled, for simultaneous control of FBPF and HPBPF tones.

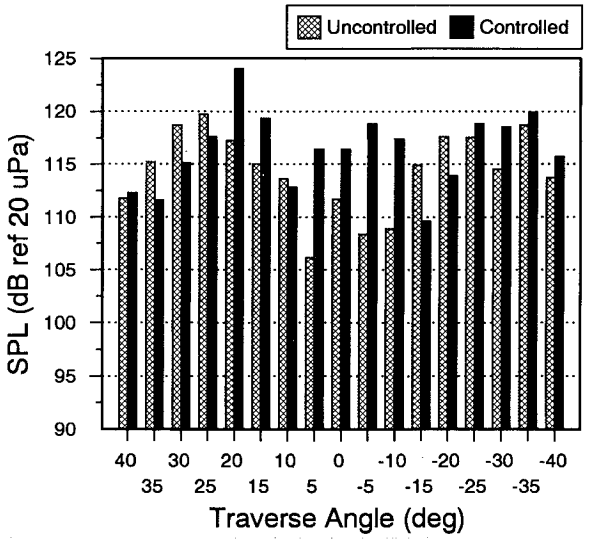

Fig. 14 Sound pressure level directivity of HPBPF tone, uncontrolled and controlled, for simultaneous control of FBPF and HPBPF tones.

The traverses of the radiated sound field are shown in Fig. 13 for the FBPF tone and in Fig. 14 for the HPBPF tone. These data were taken as the two tones were simultaneously controlled. The FBPF traverse shows reduction in a zone from −20 to +5 deg, not as good a result as when the FBPF tone was controlled singularly, but very promising. The survey of the HPBPF tone shows two zones of reduction, from −20 to −15 deg and from +25 to +35 deg. While the degree of global reduction is not large, the sideline spillover appears to be small.

Conclusions

Active control of turbofan engine inlet noise has been shown to be a promising concept by the initial results obtained on an operational engine and reported here. The multichannel control system described here has demonstrated control of the fan blade passage frequency tone, the first harmonic tone of the fan fundamental, and the blade passage frequency tone of the high-pressure compressor. The modal content of these tones consisted primarily of the plane wave, but also of higher-order modes. Reductions in tone levels of up to 16 dB are possible at single points in the far field. These reductions can be extended to sectors of up to ±30 deg about the engine axis. The area of reduction achieved is determined by the control authority of the entire system. An inlet noise control system's control authority is determined by the number of channels of control as well as the actuators and error sensors of those channels of control. The actuators must not only produce the required sound levels but must interact with the duct acoustics in such a way as to affect the propagating modes. For example, control actuators should be placed at multiple axial stations and driven by separate channels to control the higher order radial modes. The error sensors must produce information to allow stable far-field reductions as well as maximum local reduction in the area surrounding the individual error microphone so as to reduce the total number of error microphones. A system of this type with insufficient control authority will produce increased levels of the controlled tone outside the area of reduction where the controlled tone is reduced. This is the case with the current results where the levels are increased toward the sideline area such that the total tone sound power level is increased, even though a tone is reduced in an area near the axis. An optimized control system will be required to determine the level of net reduction in total tone sound power level possible.

Several features of this multichannel control system have been demonstrated and are worth noting because of their fundamental nature and the probability that they will be fundamental components in the future development of this type of turbofan engine noise control system: 1) Without changing the control sources the three channel controller produced reduced levels over an angle twice that of the single channel controller. Clearly, the number of channels of control increases the control system flexibility required to improve global reduction. 2) Far-field error sensors which are distributed in nature provide increased local areas of reduction over point sensors. In addition, they provide a steadier signal, improving the robustness of the controller. 3) Simultaneous control of two tones has been demonstrated. This shows that the parallel control approach is a promising method of controlling multiple-tone problems.

This work represents an important first step in the new area of active control of turbofan engine noise. Clearly, there are many unresolved problems which are topics of current research, such as the need for global reduction. It should be noted that perhaps reduction only in selected areas may be

sufficient, such as the reduction of noise radiated toward the ground or toward the cabin. As this technology matures, it is possible to envision a complete system installed on an aircraft turbofan engine. Reference information could be taken from very small, lightweight sensors installed on the fan and compressor stages. The distributed error microphones would be installed inside the inlet duct. An alternative error sensor approach would be to install error sensors flush with the surface on the fuselage or wing. Compact, lightweight, and high-level noise control sources would be installed around the circumference of the inlet. Several candidates for control noise sources are currently being investigated. These actuators and sensors would be linked with the active control algorithm programmed in an onboard computer.

Acknowledgments

The authors gratefully acknowledge the sponsorship of this research by the Applied Acoustics Branch and the Mission Analysis Branch of the NASA Langley Research Center. The involvement of David Chestnutt, Shelby Morris, and Carl Gerhold as technical monitors has been invaluable. The authors also greatly appreciate the contributions of Jeffrey Vipperman for work in the programming of the controllers, Christopher White and Jerry Lucas for the craftsmanlike construction of the ICD, and C. White for extensive assistance in the experimental program and construction of the high-pressure compressor reference sensor.

References

[1]Owens, R. E., "Energy Efficient Engine Propulsion System—Aircraft Integration Evaluation," NASA CR-159488, 1979.

[2]Hanson, D. B., "A Study of Subsonic Fan Noise Sources," AIAA 2nd Aeroacoustics Conf., AIAA Paper 75-468, Hampton, VA, March 1975.

[3]Hubbard, H. H. (ed.), *Aeroacoustics of Flight Vehicles,* NASA Reference Pub. 1258, Aug. 1991.

[4]Preisser, J. S., Schoenster, J. A., Golub, R. A., and Horne, C., "Unsteady Fan Blade Pressure and Acoustic Radiation from a JT15D-1 Turbofan Engine at Simulated Forward Speed," AIAA 19th Aerospace Sciences Meeting, AIAA Paper 81-0096, Jan. 1981.

[5]Majjigi, R. K., and Gliebe, P. R., "Development of a Rotor Wake Vortex Model," NASA CR-174849, 1984.

[6]Ng, W. F., O'Brien, W. F., and Olsen, T. L., "Experimental Investigation of Unsteady Fan Flow Interaction with Downstream Struts," AIAA Paper 86-1970, July 1986.

[7]Kaji, S., Okazaki, T., "Propagation of Sound Waves Through a Blade Row," *Journal of Sound and Vibration,* Vol. 11, No. 3, March 1970.

[8]Mani, R., "Discrete Frequency Noise Generation From an Axial Flow Fan Blade Row," *Journal of Basic Engineering,* Vol. 92, Series D, No. 1, 1970.

[9]Kantola, R. A., and Gliebe, P. R., "Effects of Vane/Blade Ratio and Spacing on Fan Noise," AIAA Paper 81-2033, Oct. 1981.

[10]Taylor, A. C., and Ng, W. F., "Analytical Prediction of the Unsteady Lift on a Rotor Caused by Downstream Struts," American Society of Mechanical Engineers Paper 87-GT-145, May–June 1987.

[11]Simorich, J. C., Lavrich, P. L., Sofrin, T. G., and Topol, D. A., "Active Aerodynamic Control of Wake-Airfoil Interaction Noise—Experiment," DGLR/AIAA Paper 92-02-038, 1992.

[12]Lueg, P., "Process of Silencing Sound Oscillations," US Patent 2.043.416, 1934.

[13]Widrow, B., et al., "Adaptive Noise Canceling: Principles and Applications," *Proceedings of the Institute of Electrical and Electronics Engineers,* Vol. 63, No. 12, Dec. 1975, pp. 1692–1716.

[14]Ffowcs Williams, J. E., "Anti-Sound," *Proceedings of the Royal Society of London,* A395, 1984, pp. 63–88.

[15]Fuller, C. R., Roger, C. A., and Robertshaw, H. H., "Active Structural Acoustic Control with Smart Structures," *Proceedings of the Society of Photo-Optical Instrumentation Engineers Conference 1170 on Fiber Optic Smart Structures and Skins II,* 1989, pp. 338–358.

[16]Elliot, S. J., and Nelson, P. A., "The Active Control of Sound," *Electronics and Communication Engineering Journal,* Aug. 1990, pp. 127–136.

[17]Widrow, B., and Hoff, M., "Adaptive Switching Circuits," *IRE WESCON Conv. Rec.,* Pt. 4, 1960, pp. 96–104.

[18]Widrow, B., "Adaptive Filters," *Aspects of Network and System Theory,* edited by R. Kalman and N. DeClaris, Rinehart and Winston, New York, 1971, pp. 563–587.

[19]Burdisso, R. A., Thomas, R. H., Fuller, C. R., and O'Brien, W. F., "Experiments on the Active Control of Inlet Fan Noise From A JT15D Engine," 122nd Meeting of the Acoustical Society of America, Houston, TX, Nov. 1991.

[20]Thomas, R. H., Burdisso, R. A., Fuller, C. R., and O'Brien, W. F., "Preliminary Experiments on Active Control of Fan Noise from a JT15D Turbofan Engine," *Journal of Sound and Vibration,* Vol. 161, No. 3, 1993, pp. 532–537.

[21]Burdisso, R. A., Thomas, R. H., Fuller, C. R., and O'Brien, W. F., "Active Control of an Acoustic Spinning Mode From a Turbofan Engine," 124th Meeting of the Acoustical Society of America, New Orleans, LA, Nov. 1992.

[22]Preisser, J. S., Schoenster, J. A., Golub, R. A., and Horne, C., "Unsteady Fan Blade Pressure and Acoustic Radiation From a JT15D-1 Turbofan Engine at Simulated Forward Speed," AIAA Paper 81-0096, Jan. 1981.

[23]Preisser, J. S., and Chestnutt, D., "Flight Effects on Fan Noise with Static and Wind-Tunnel Comparisons," *Journal of Aircraft,* Vol. 21, No. 7, 1984, pp. 453–461.

[24]Joppa, P. D., "Acoustic Mode Measurements in the Inlet of a Turbofan Engine," *Journal of Aircraft,* Vol. 24, No. 9, 1987, pp. 587–593.

[25]Homyak, L., McArdle, J. G., and Heidelberg, L. J., "A Compact Inflow Control Device for Simulating Flight Fan Noise," AIAA Paper 83-0680, April 1983.

[26]Tyler, J. M., and Sofrin, T. G., "Axial Flow Compressor Noise Studies," *Society of Automotive Engineers Transactions,* No. 70, 1962, pp. 309–332.

[27]Heidmann, M. F., Saule, A. V., and McArdle, J. G., "Analysis of Radiation Patterns of Interaction Tones Generated by Inlet Rods in the JT15D Engine," AIAA Paper 79-0581, March 1979.

[28]Widrow, B., and Stearns, S. D., *Adaptive Signal Processing,* Prentice-Hall, Englewood Cliffs, NJ, 1985.

[29]Oppenheim, A. V., and Schafer, R. W., *Digital Signal Processing,* Prentice-Hall, Englewood Cliffs, NJ, 1975.

[30]Nelson, P. A., Sutton, T. J., and Elliot, S. J., "Performance Limits for the Active Control of Random Sound from Multiple Primary Sources," *Proceedings of the IOA Spring Conference,* Southhampton, 1990.

[31]Elliott, S. J., Stothers, I. M., and Nelson, P. A., "A Multiple Error LMS Algorithm and its Application to the Active Control of Sound and Vibration," *Institute of Electrical and Electronics Engineers Transactions on Acoustics, Speech, and Signal Processing,* Vol. ASSP-35, No. 10, 1987.